Electronic Supplementary Information

Donor atom selective coordination of Fe^{3+} and Cr^{3+} trigger fluorophore specific emission in a rhodamine-naphthalimide dyad

Narendra Reddy Chereddy,*[a,b] Krishnan Saranraj,[a] Ayan Kumar Barui,[c] Chitta Ranjan Patra*[c], Vaidya Jayathirtha Rao*[b] and Sathiah Thennarasu*[a]

[a]*Organic Chemistry Division, CSIR-Central Leather Research Institute, Adyar, Chennai-600 020, India.*

[b]*Crop Protection Chemicals,* [c]*Biomaterials Group, CSIR-Indian Institute of Chemical Technology, Tarnaka, Hyderabad-500 007, India.*

chereddynarendra@gmail.com; thennarasu@gmail.com

Table of contents **Page**

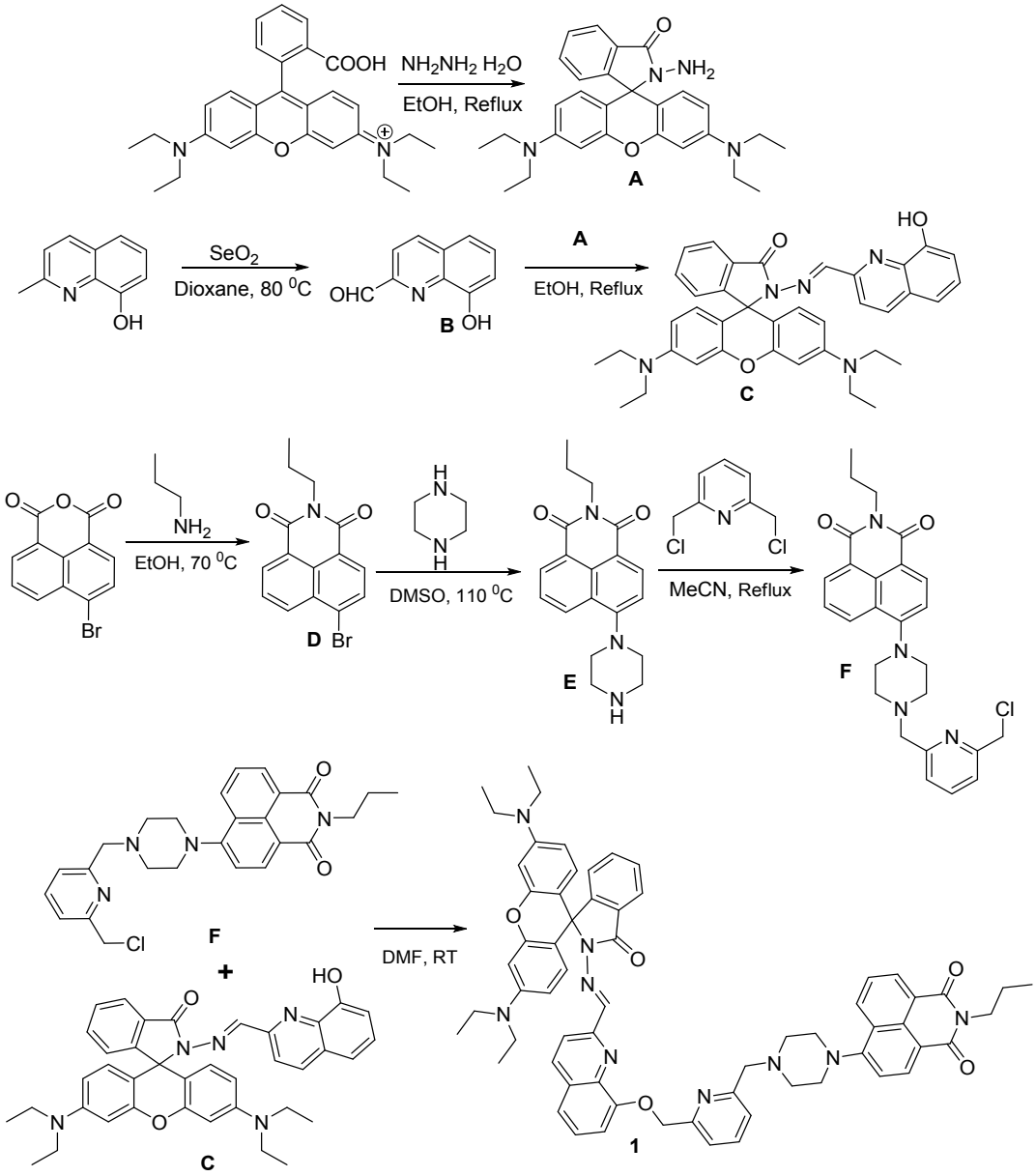

Scheme: Synthesis of rhodamine-naphthalimide dyad **1**

Experimental Procedure

General Information

Dry acetonitrile and double distilled water were used in all experiments. All the materials for synthesis were purchased from commercial suppliers and used without further purification. The human lung carcinoma cells (A549) and Chinese hamster ovarian cells (CHO) and ECV-

304 cells were purchased from American Type Culture Collection (Manassas, VA). ECV-304 cells were a donation from Chair, Dr. V. Shah, Gastroenterology and Hepatolog Department, Mayo Clinic, Rochester, MN, USA. Dulbecco's Modified Eagle Medium (DMEM), Dulbecco's Phosphate Buffered Saline (DPBS), Hank's Balanced Salt Solution (HBSS), Fetal Bovine Serum (FBS), penicillin/streptomycin and Hoechst 33258 were purchased from Sigma-Aldrich, USA. The solutions of metal ions were prepared from the corresponding chloride salts. Absorption spectra were recorded on a SPECORD 200 PLUS UV-visible spectrophotometer. Fluorescence measurements were performed on a Cary Eclipse fluorescence spectrophotometer (Excitation wavelength 400 nm; Slit width 5 nm). Fluorescence quantum yields were calculated using rhodamine 6G as standard as previously reported.[11] All pH measurements were made with a Systronics μpH System Model 361. NMR spectra were recorded using a Bruker Avance 400 MHz spectrometer operated at 400 MHz. ESI-HRMS spectrum was obtained on a Thermo exactive PE Sciex API3000 mass spectrometer. All measurements were carried out at room temperature. Stock solutions of the probe were prepared by dissolving 10.38 mg of **1** in 1:1 v/v 0.01M Tris HCl-CH_3CN (pH 7·4) and making up to the mark in a 10 mL volumetric flask. Further dilutions were made to prepare 10 μM solutions for the experiments. Stock solutions of metal ions (1 M) were prepared in de-ionised water.

Synthesis of rhodamine hydrazide (A)

Rhodamine hydrazide was synthesized according to the reported procedure. [12]

Synthesis of probe 1

Probe **1** was synthesized in a multi-step procedure. To a solution of SeO_2 (1.66 g, 15 mmol) in 1,4-dixane (20 mL) under N_2 atmosphere, 2-methyl 8-quinolinol (1.59 g, 10 mmol) in 1,4-dixane (20 mL) was added drop wise, the resulted mixture was allowed to stir for 8h under N_2

atmosphere at 70^0 C and progress of the reaction was monitored by TLC. After the completion of reaction, the reaction mixture was allowed to cool to room temperature, filtered and subjected silica gel 100-200 mesh column chromatography using 95:5 hexane-ethyl acetate as eluent to get 0.87 g (50%) of 8-hydroxyquinoline 2-aldehyde (**B**) in pure form as yellow colour solid. To a solution of **B** (0.44 g, 2.5 mmol) in ethanol (20 mL), rhodamine hydrazide, **A**, (0.9 g, 2.0 mmol) was added and the mixture was refluxed for ~6h. After completion of the reaction, reaction mixture was cooled to room temperature, concentrated and subjected to column chromatography to obtain **C** (0.92 g, 75%) as white solid. To a solution of 4-bromo-1,8-naphthanoic anhydride (1.00 g, 3.60 mmol) in ethanol maintained at 70 ^{0}C, propylamine (1.0 mL) was added slowly. The resulting mixture was stirred for ~1h, cooled to room temperature and precipitate formed (**D**) was filtered, used in the next step. To this product **D**, (0.70 g, 2.20 mmol) in DMSO, piperazine (1.00 g, 11.6 mmol) and K_2CO_3 (0.42 g, 3.0 mmol) were added and stirred at 110 ^{0}C for 3h. After completion, the reaction mixture was extracted with DCM and subjected to column chromatography (silica gel 100-200 mesh) and eluted using ethtyl acetate to get 0.50 g (70%) of **E**. To 4-piperazinyl-N-propyl-1,8-naphthanamide, **E**, (0.48 g, 1.5 mmol) in acetonitrile (20 mL), 2,6-Bis(chloromethyl)pyridine (0.71 g, 4.0 mmol) was added and the mixture was refluxed overnight under N_2 atmosphere. After completion of the reaction, the reaction mixture was cooled to room temperature, concentrated and subjected to column chromatography (silica gel 100-200 mesh, 1:9 ethyl acetate-hexane as eluent) to afford **F** (0.44 g, 64%) as pale yellow solid. To the mixture of **C** (0.61 g, 1.0 mmol) and potassium carbonate (0.28 g, 2.0 mmol) in DMF, **F** (0.51 g, 1.1 mmol) was added and the mixture was stirred at room temperature over night. After completion, the reaction mixture was partitioned between chloroform and water, chloroform layer was collected. The aqueous layer was washed thrice with chloroform (3 x 10 mL) and the combined organic extract was washed with brine,

concentrated and subjected to column chromatography to afford **1** in pure form (0.60 g, 58%). ^{1}H NMR ($CDCl_3$, 400 MHz), δ (ppm): 1.01 (t, *J* = 7.3 Hz, 3H, $NCH_2CH_2\underline{CH_3}$), 1.13 (t, *J* =6.7 Hz, 12H, $NCH_2\underline{CH_3}$), 1.76 (m, 2H, $NCH_2\underline{CH_2}CH_3$), 2.90 (s, 4H, Piperazine CH_2), 3.35-3.38 [m, 12H, $N\underline{CH_2}CH_3$ (8H) and Piperazine CH_2 (4H)], 3.88 (s, 2H, Pyridine $\underline{CH_2}$), 4.14 (t, *J* = 7.4 Hz, 2H, $N\underline{CH_2}CH_2CH_3$), 5.48 (s, 2H, $O\underline{CH_2}$), 6.25 (d, *J* = 8.9 Hz, 2H, Xanthene-H), 6.48 (s, 2H, Xanthene-H), 6.57 (d, *J* = 8.8 Hz, 2H, Xanthene-H), 7.04 (d, *J* = 5.3 Hz, 1H, Ar-H), 7.17 (d, *J* = 7.1 Hz, 1H, Ar-H), 7.22 (d, *J* = 8.1 Hz, 1H, Ar-H), 7.33 (m, 2H, Ar-H), 7.42-7.56 (m, 3H, Ar-H), 7.65-7.74 (m, 2H, Ar-H), 7.80 (t, *J* = 7.6 Hz, 1H, Ar-H), 8.00 (m, 2H, Ar-H), 8.09 (d, *J* = 8.6 Hz, 1H, Ar-H), 8.41 (d, *J* = 8.4 Hz, 1H, Ar-H), 8.52 (d, *J* = 7.8 Hz, 1H, Ar-H), 8.58 (d, *J* = 7.2 Hz, 1H, Ar-H), 9.10 (s, 1H, Imine-H). ^{13}C NMR ($CDCl_3$, 100 MHz), δ (ppm): 11.6, 12.6, 21.4, 41.8, 44.3, 52.9, 53.3, 64.3, 66.4, 71.5, 98.1, 106.1, 108.0, 110.3, 114.9, 116.8, 118.9, 120.2, 121.6, 122.3, 123.3, 123.6, 124.0, 125.7, 126.1, 127.0, 127.9, 128.4, 128.9, 129.5, 129.9, 130.3, 131.1, 132.6, 133.7, 135.8, 137.5, 139.9, 148.4, 148.9, 151.8, 153.3, 154.0, 154.2, 155.9, 157.0, 157.1, 164.1, 164.55, 165.18; ESI-HRMS (+ve mode, m/z): 1038.49759 ($M+H^+$), Calc. for $C_{64}H_{64}N_9O_5$ is 1038.50304.

Sample preparation for cell culture

The solution of **1** was prepared in sterile DMSO solvent with stock solution concentrations of 10 mM. Similarly, 10 mM stock solutions of Fe^{3+} and Cr^{3+} salts were prepared in sterile Millipore water. The freshly prepared stock solutions of each sample were used for cell culture experiment.

Cell culture experimentation

A549, CHO and ECV-304 cells were maintained in DMEM complete media, supplemented with 10% Fetal Bovine Serum (FBS) and 1% penicillin/streptomycin at 37 ^{0}C humidified incubator with 5% CO_2. Cells with 70% confluence were seeded onto 96-well-plate, and 24-

well-plate for cytotoxicity assays and fluorescence microscopy studies, respectively.

MTT assay

The MTT (3-(4,5-dimethylthiazol-2-yl)-2,5-diphenyl tetrazolium bromide) assay has been used to measure the activity of enzymes that reduce MTT to formazan dyes, giving rise to a purple colour.[13-15] Briefly, 10,000 of A549, and ECV-304 cells were plated in each well of a 96-well tissue culture plate with 100 μL of complete DMEM media at 37 ^{0}C humidified incubator with 5% CO_2 for 24 h. Next day, the media was replaced with 100 μL (in each well) fresh media and the cells were incubated with probe **1** at different concentrations (0.1-20 μM) for another 48 h. 1 mL of MTT stock solution (5 mg/mL) was diluted to 10 mL using complete DMEM media and 100 μL of the diluted MTT solution was added to each well of 96 well plate by replacing the old media and allowed to incubate for 4 h. After that, the media in each well was replaced by 100 μL of 1:1 DMSO-Methanol mixture (v/v) for solubilizing the purple formazan product. Then, the plate was kept on a shaker for homogeneous mixture of the solution. Finally, the microplate reader (ELx 800 MS) has been used to measure the absorbance of solution in each well of the plate at 570 nm.

Fluorescence microscopy

To detect the Fe^{3+} and Cr^{3+} in both cancerous and non-cancerous cells, A549 and CHO cells were seeded at $2x10^4$ cells/mL/well in a 24-well tissue culture plate for 24 h at 37 ^{0}C humidified incubator with 5% CO_2 in complete DMEM media. After 24 h, the cells were incubated with 20 μM of probe **1** for another 4 h. The cells were thoroughly washed with DPBS for six times to eradicate the unbound probe **1** from the surface of cell membrane. After that, the cells treated with probe **1** were either incubated with 50 μM Fe^{3+} or with 50 μM Cr^{3+} for 1 h. Additionally, cells were also treated with only **1** (20 μM), only Fe^{3+} (50 μM) and only Cr^{3+} (50 μM) solutions and again washed with DPBS for six times to remove the

remaining Fe^{3+} and Cr^{3+} materials respectively. Finally, the cells were stained with 2.5 μg/mL of Hoechst 33258 solution (for staining of nucleus) for 30 minutes and washed three times with DPBS. The fluorescence images of A549 and CHO cells treated with probe **1** and Fe^{3+}, probe **1** and Cr^{3+}, only probe **1**, only Fe^{3+} and only Cr^{3+} were observed under fluorescence microscope (Nikon Eclipse: TE 2000-E, Japan) through excitation of 488 nm and emission of 525 nm for green fluorescence and excitation of 518 nm and emission of 605 nm for red fluorescence. Hoechst stained A549 and CHO cells were observed through the blue channel with an excitation of 340 nm and emission of 435 nm.

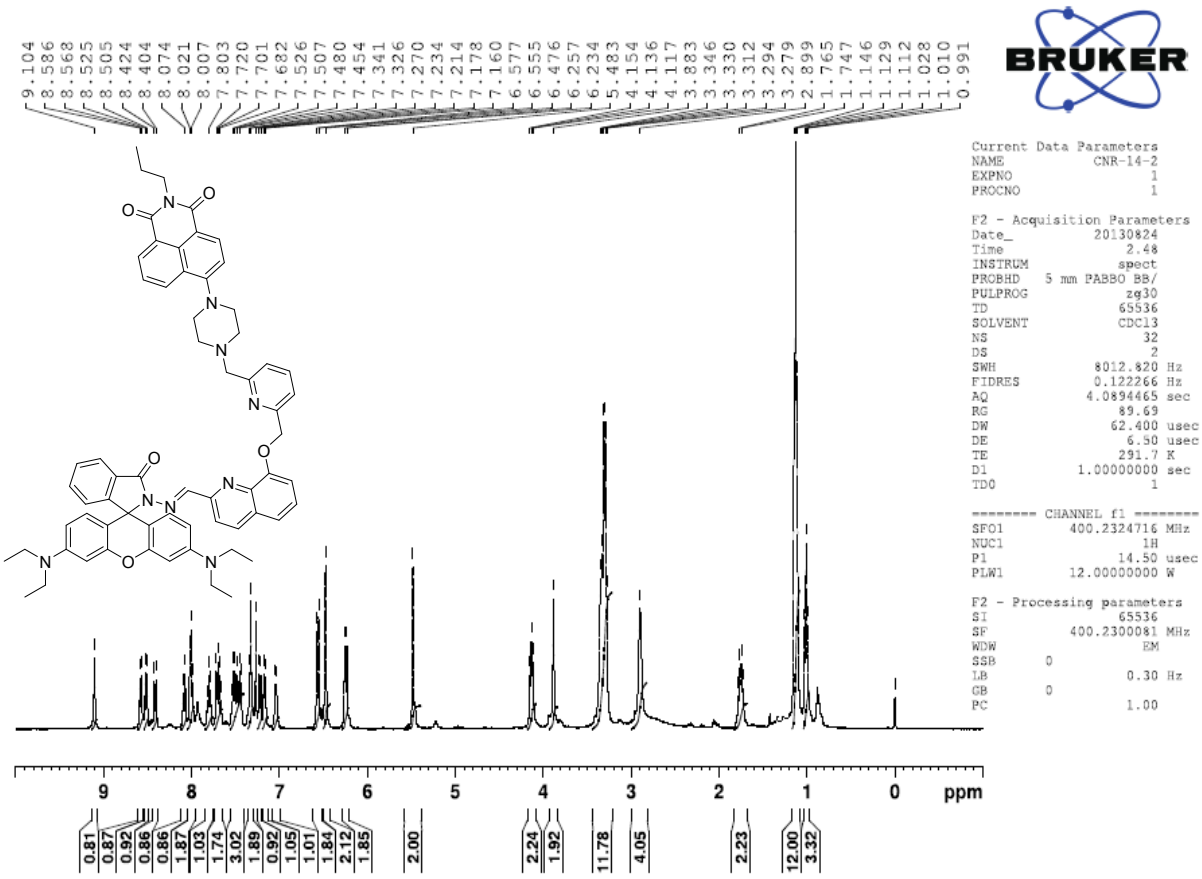

Fig. S1. ^{1}H NMR spectrum of **1** in $CDCl_3$

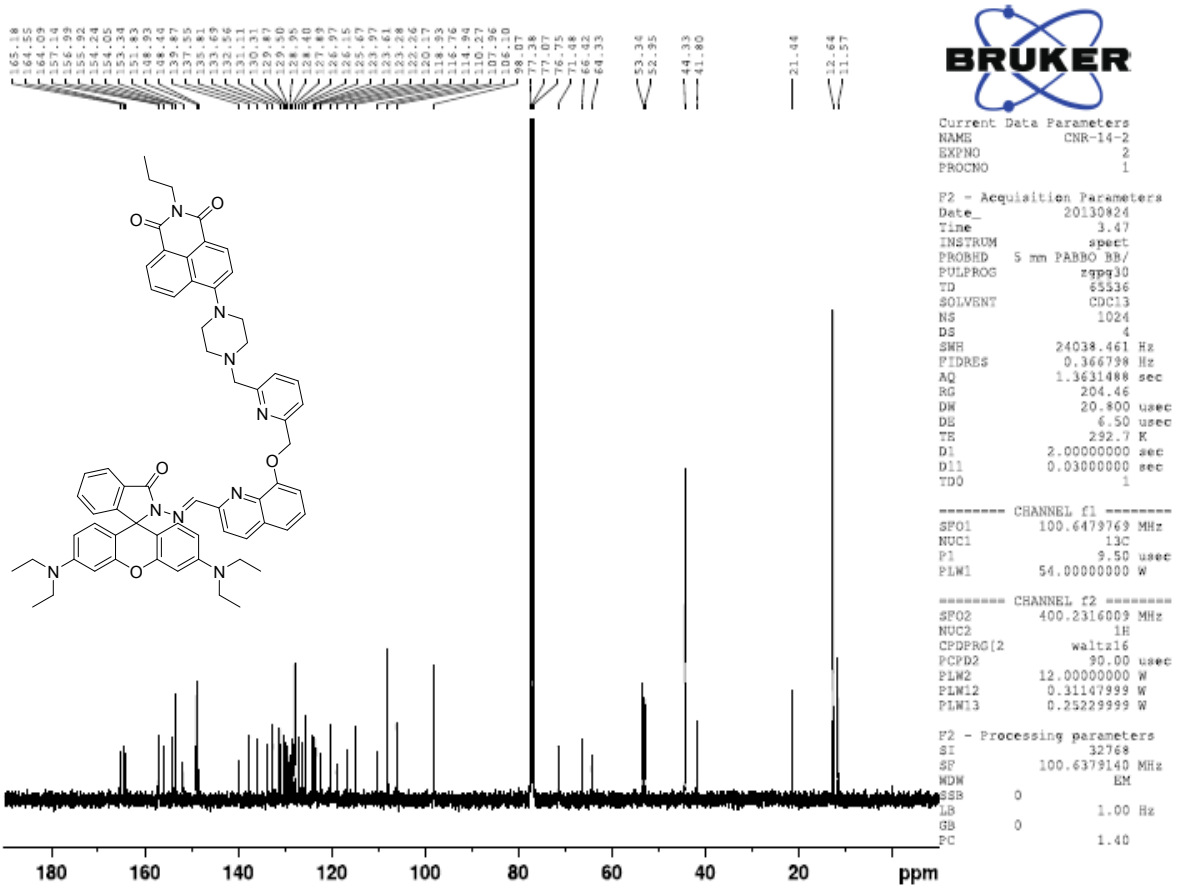

Fig. S2. ^{13}C NMR spectrum of **1** in $CDCl_3$

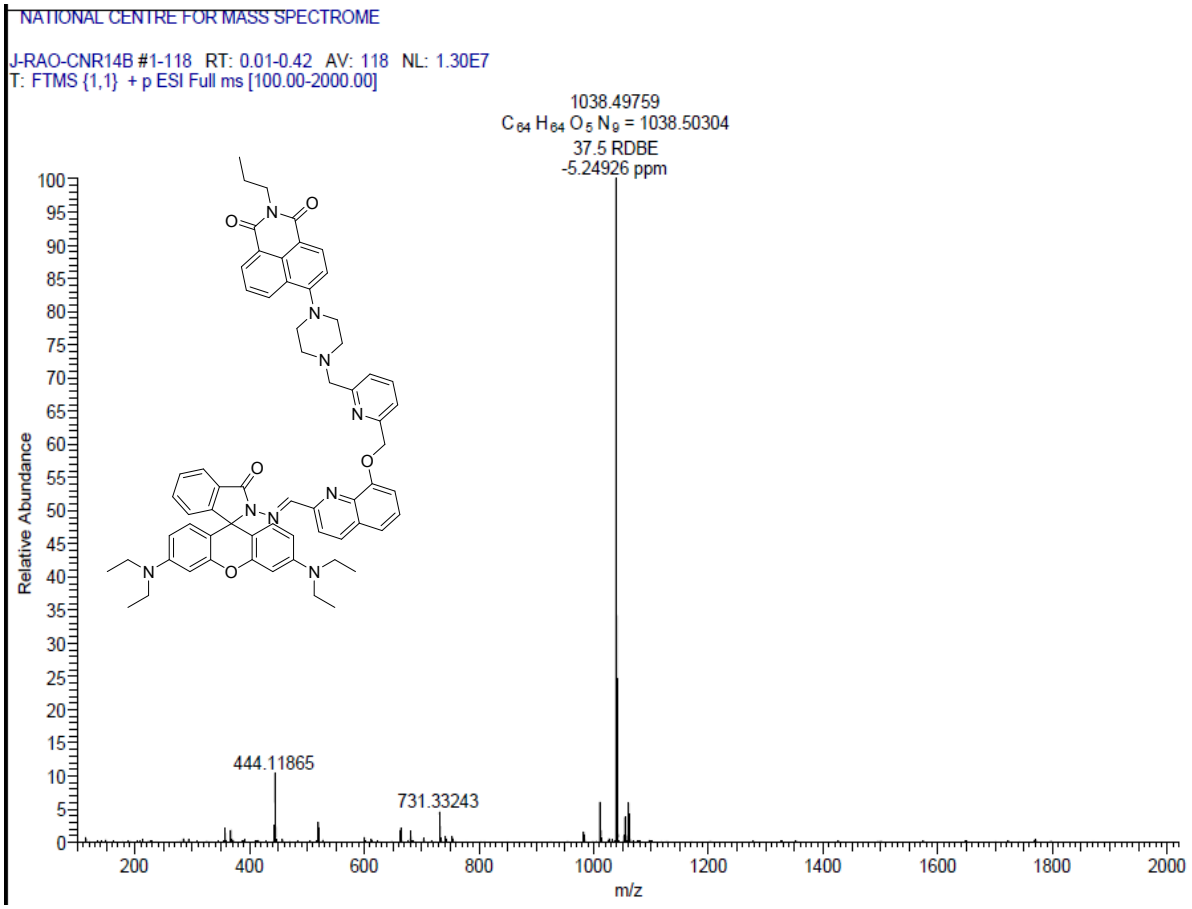

Fig. S3. ESI Mass spectrum of **1**

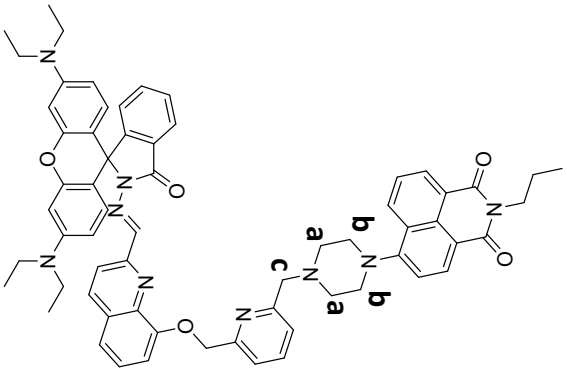
a
b
c
q

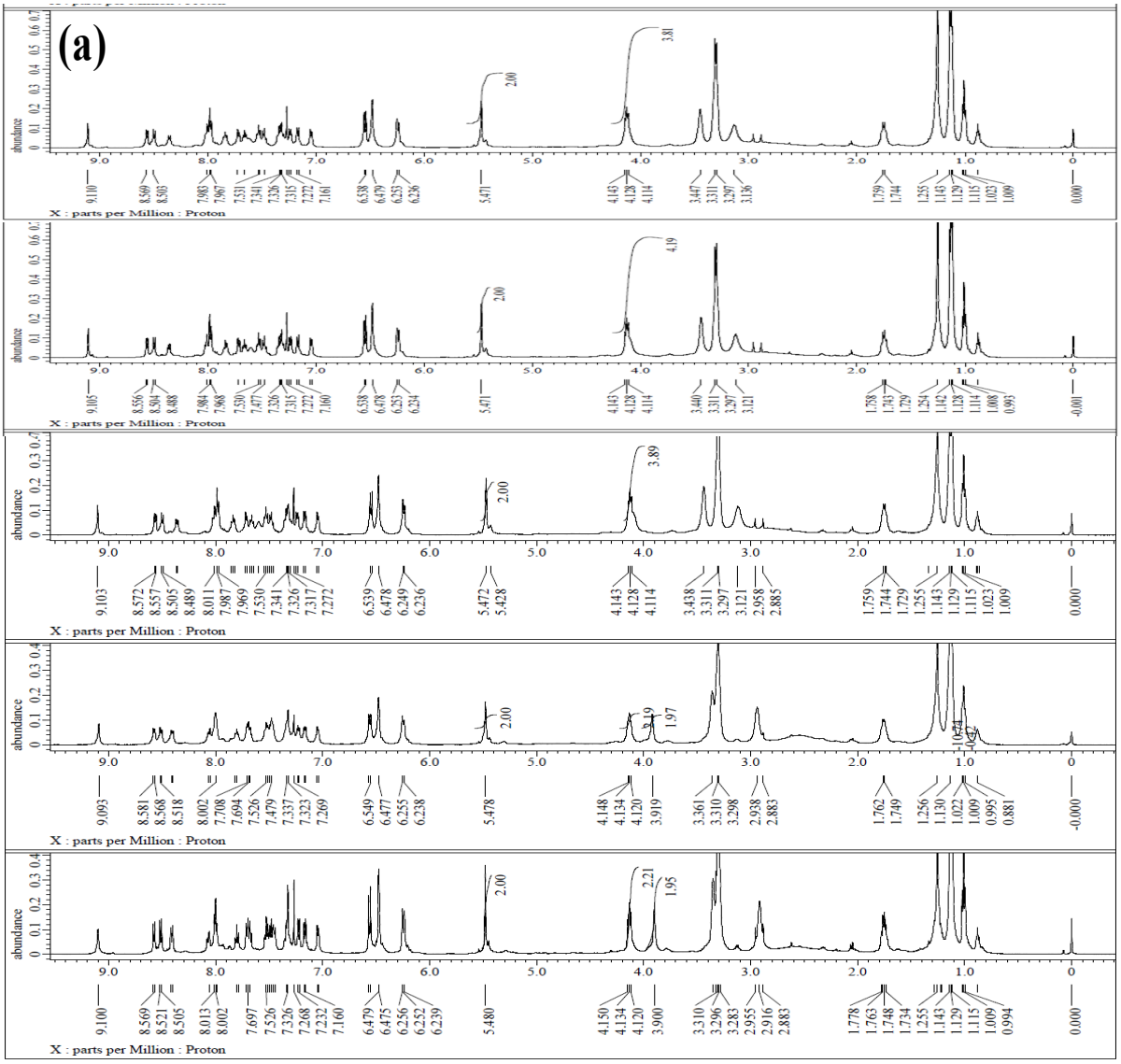
(a)
abundance
X : parts per Million : Proton

(b)

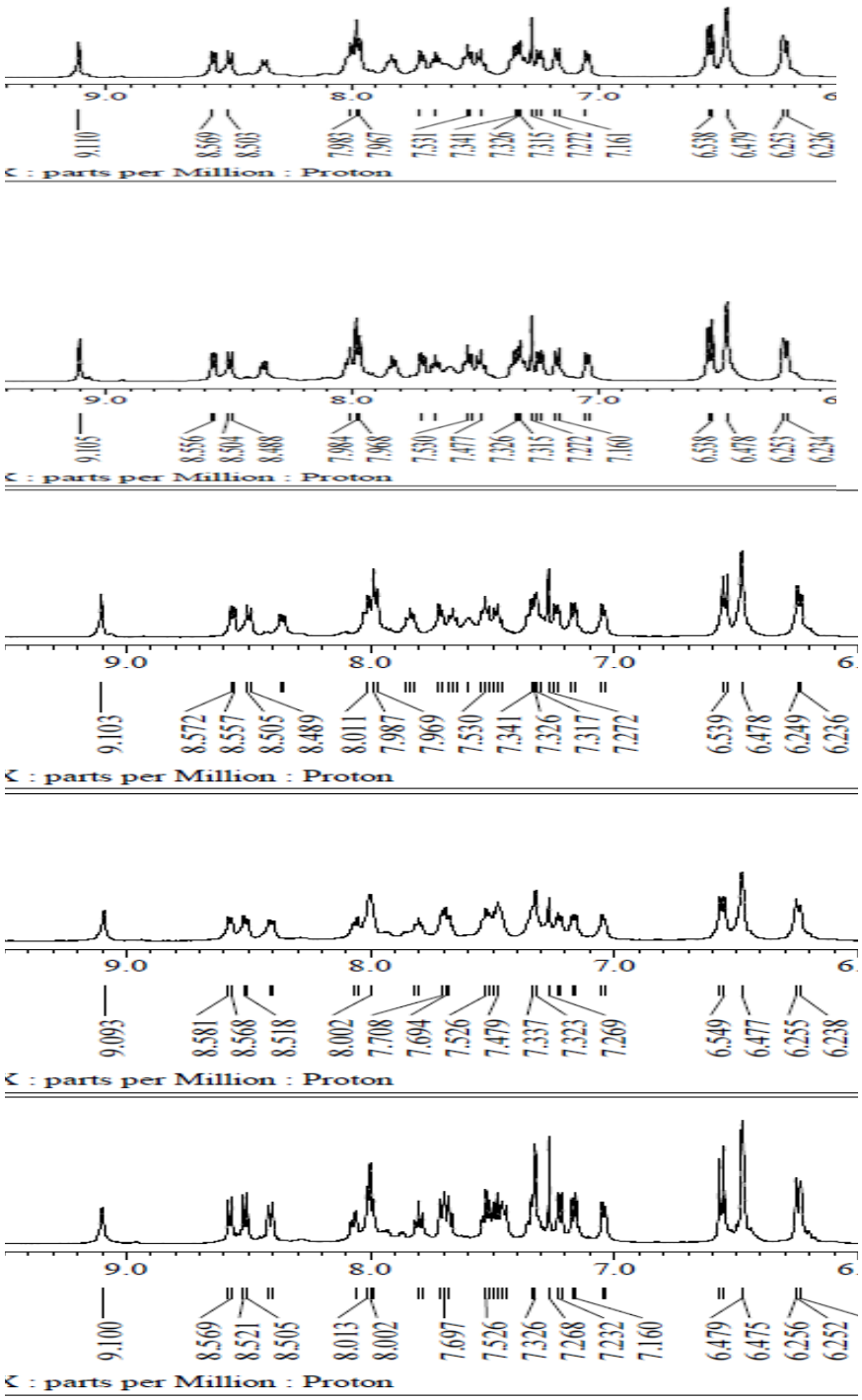

Fig. S4. ^{1}H NMR spectra full (**a**) and expanded aromatic region (**b**) of **1** in the presence of Cr^{3+} (from bottom to top): **1** alone, **1** with 1.0 equivalent of Cr^{3+}, **1** with 2.0 equivalents of Cr^{3+}, **1** with 3.0 equivalents of Cr^{3+} and **1** with 4.0 equivalents of Cr^{3+}

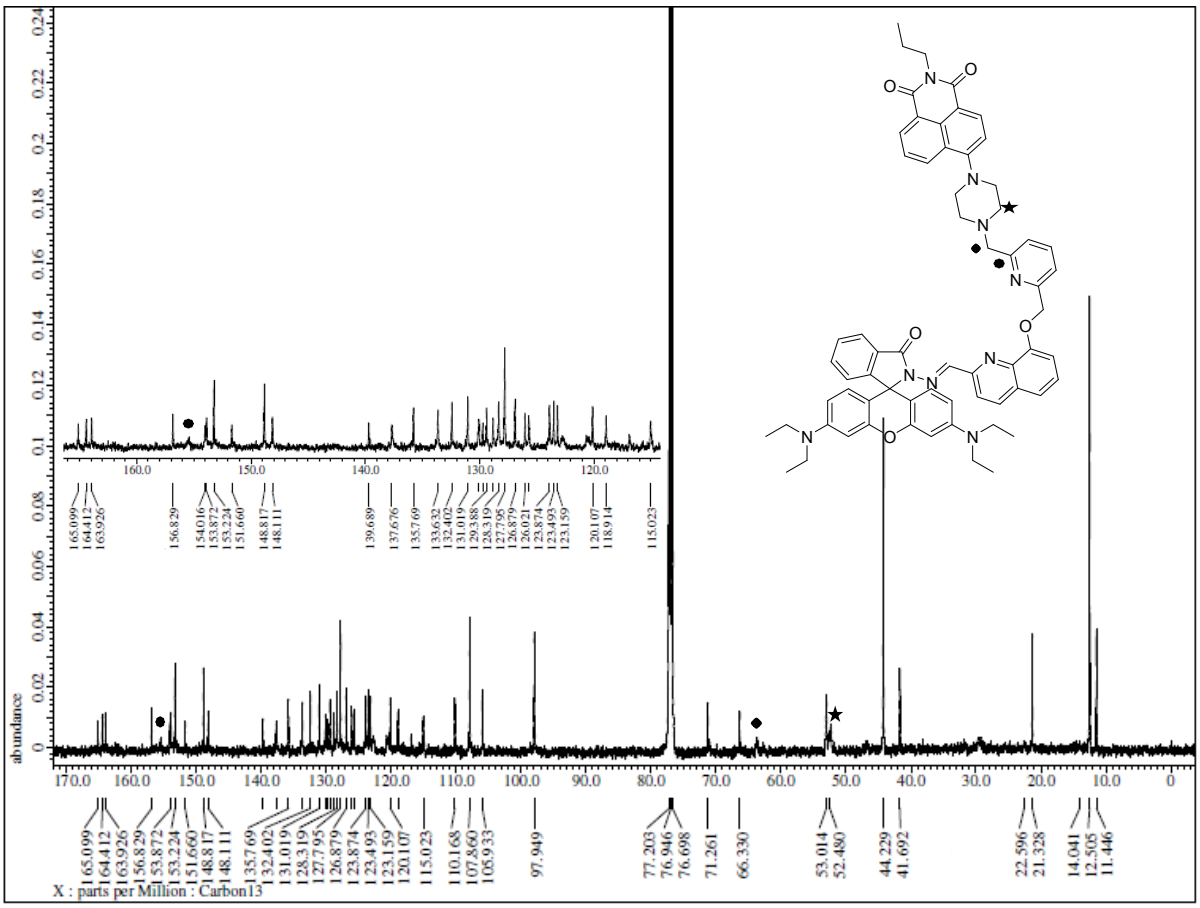

Fig. S5. ^{13}C NMR spectrum of **1** with 4.0 equivalents of Cr^{3+}

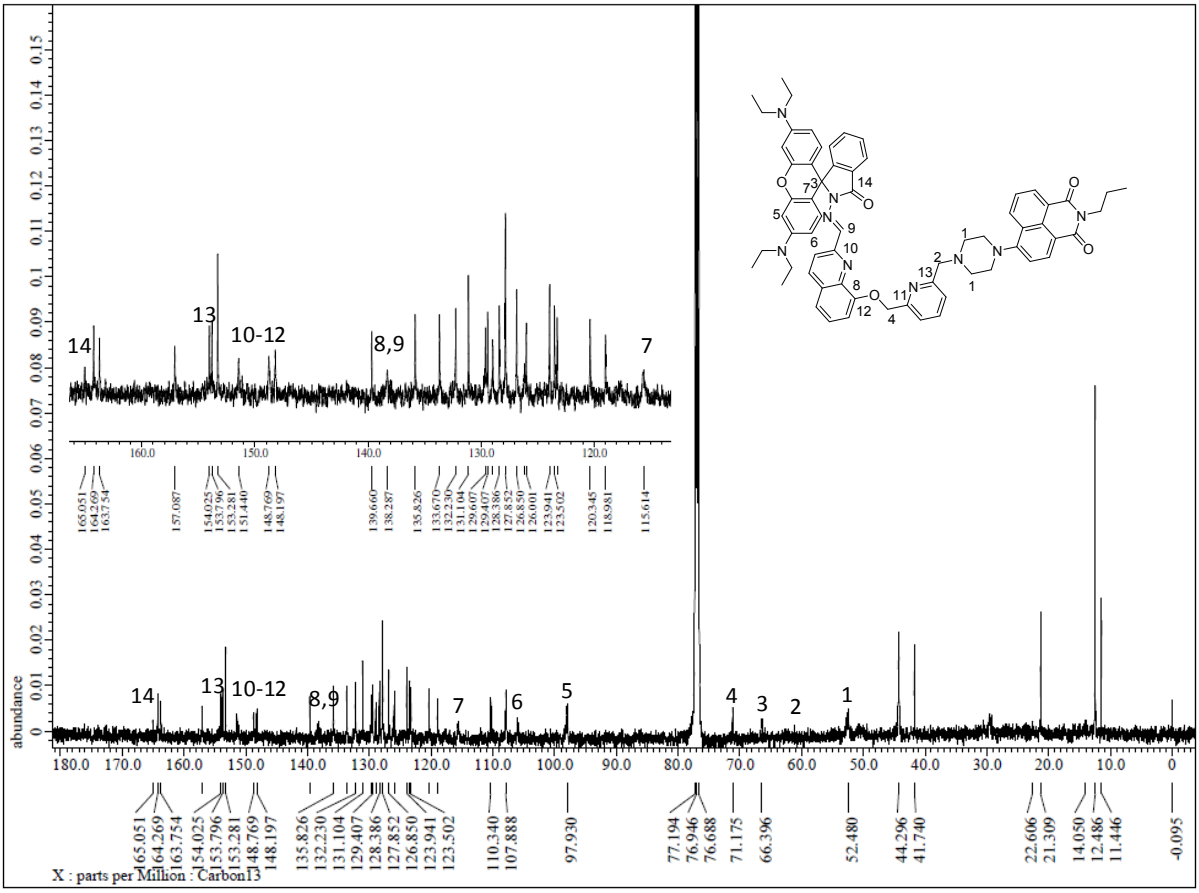

Fig. S6. ^{13}C NMR spectrum of **1** with 1.0 equivalents of Fe^{3+}

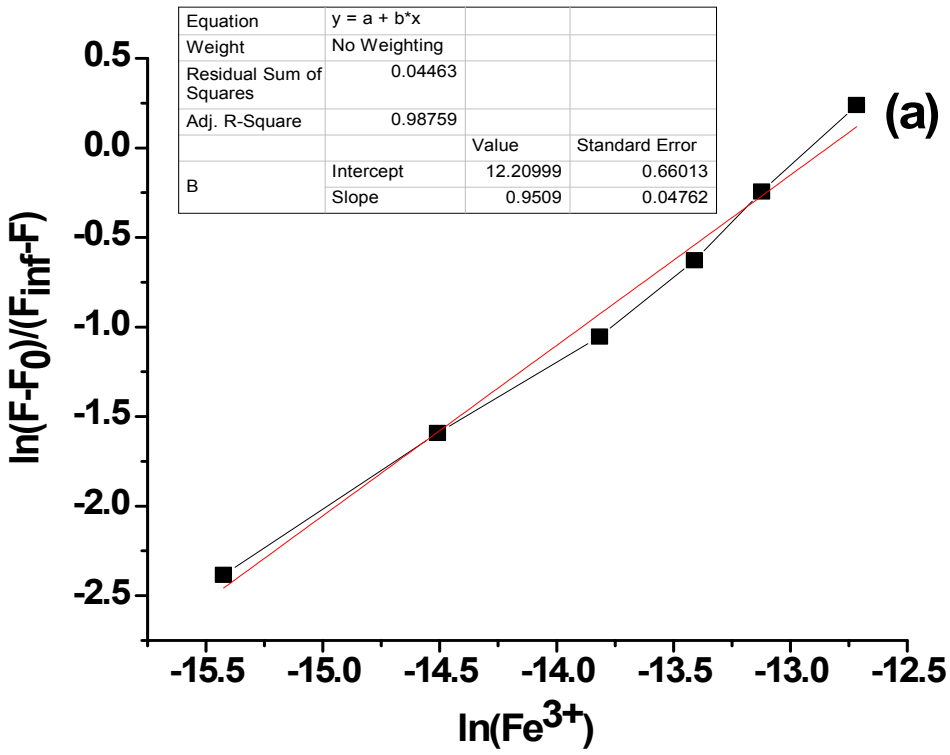

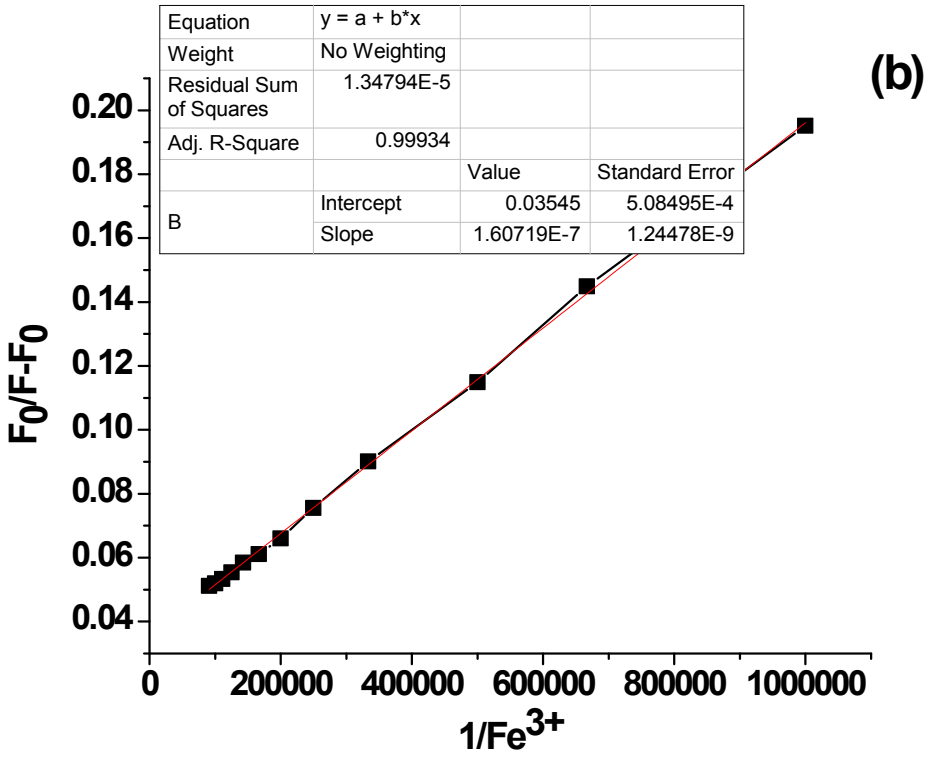

Fig. S7. Plot of ln[(F-F0)/(F_{inf}-F)] against ln(Fe^{3+}); the stoichimetry of **1-Fe^{3+}** obtained directly from the slope, is 0.9509 ≅ 1 (**a**) and Benesi–Hildebrand plot for determination of binding constant (**b**).

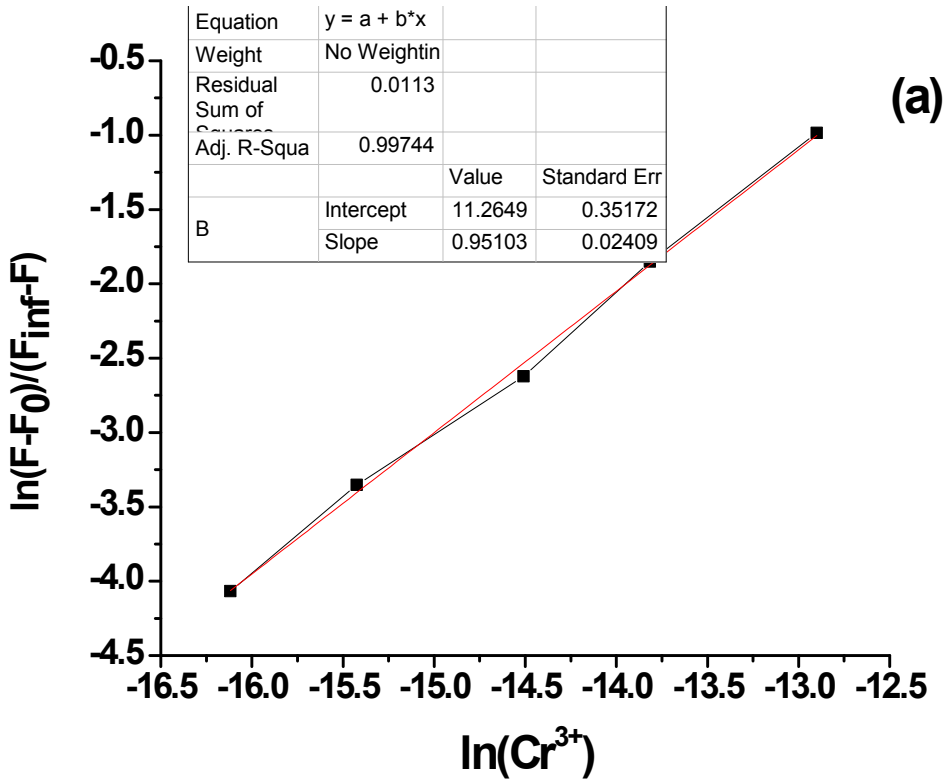

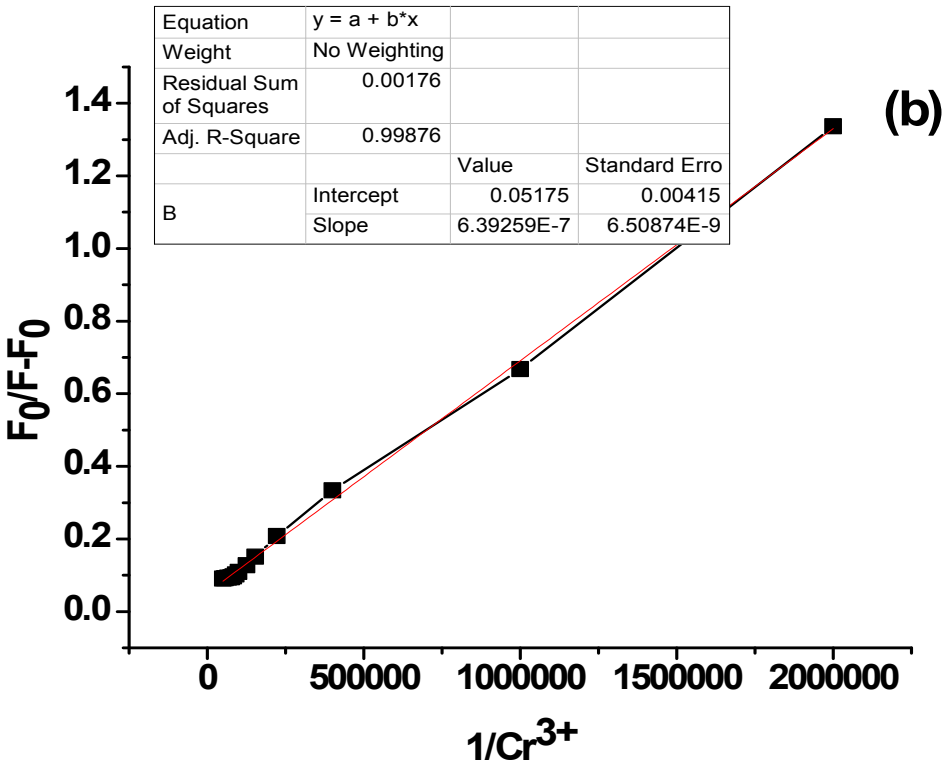

Fig. S8. Plot of ln[(F-F0)/(F_{inf}-F)] against ln(Cr^{3+}); the stoichimetry of **1-Cr^{3+}** obtained directly from the slope, is 0.9510 ≅ 1 (**a**) and Benesi–Hildebrand plot for determination of binding constant (**b**).

Table S1. Comparison of **1** with the reported chemosensors

Sensor	Target metal ion	Limit of Detection	Signalling moiety
Ref 1	Fe^{3+}	0.6 ppm	Rhodamine
Ref 2	Fe^{3+}	0.4 ppm	Rhodamine
Ref 3	Fe^{3+}	3.0 ppm	Rhodamine
Ref 4	Fe^{3+}	1.0 ppb	Rhodamine
Ref 5	Fe^{3+}	5.4 ppb	Rhodamine
Present	Fe^{3+}	0.6 ppb	Rhodamine/naphthalimide
Ref 6	Cr^{3+}	60 ppb	pyrene
Ref 7	Cr^{3+}	11 ppb	naphthalimide
Ref 8	Cr^{3+}	6.0 ppm	Au nano particles
Ref 9	Cr^{3+}	0.27 ppm	spirobenzopyran
Ref 10	Cr^{3+}	0.14 ppm	Fluorescein
Present	Cr^{3+}	10.8 ppb	Rhodamine/naphthalimide

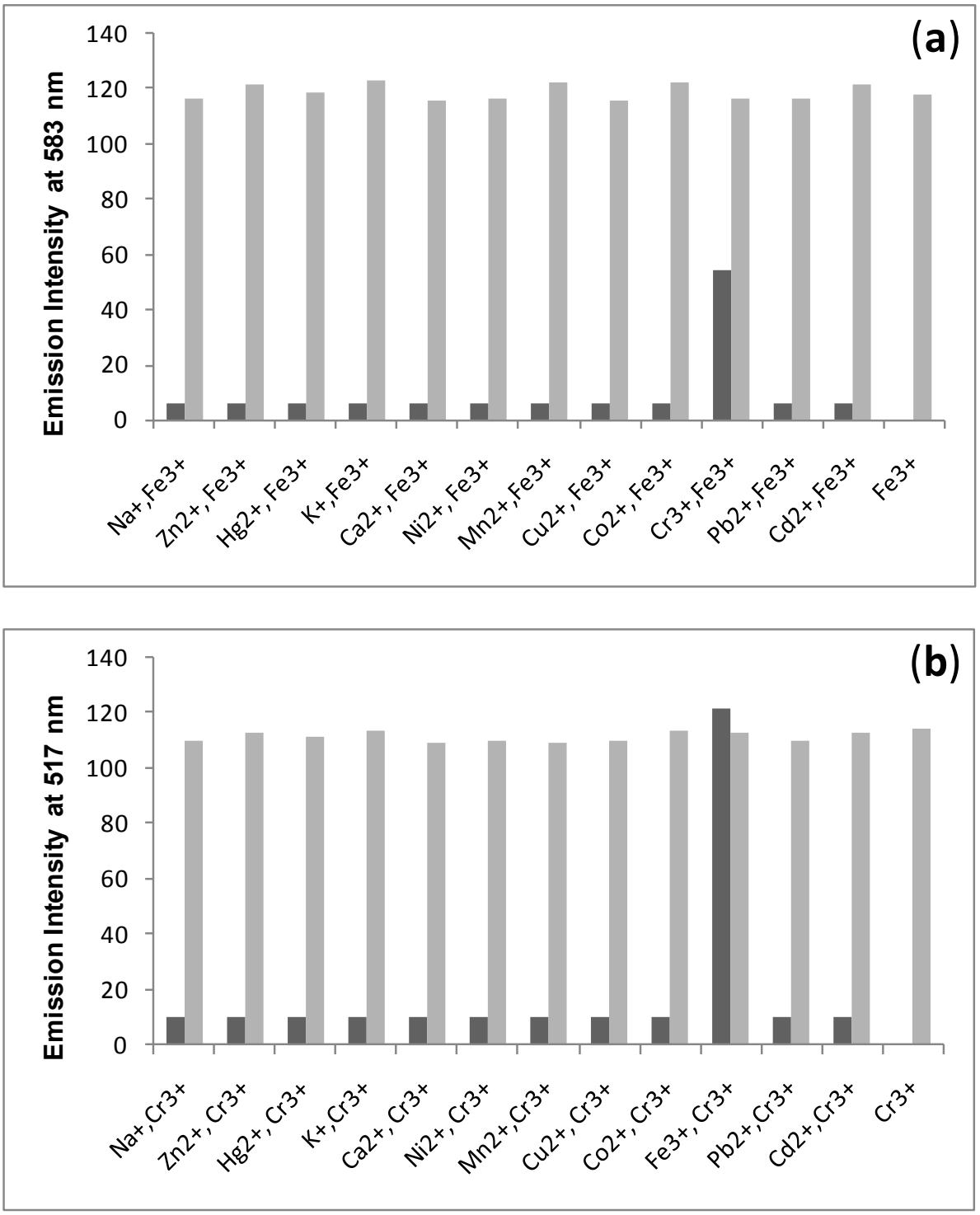

Fig. S9. Metal-ion selectivity of **1** in 1:1 v/v 0.01M Tris HCl-CH_3CN, pH 7.4. The dark bars represent the fluorescence emission at ~580 nm of a solution of **1** (10 μM) and 2 equiv of other metal ions. The light bars show the the fluorescence emission at ~583 nm after the addition of 2 equiv of Fe^{3+} (**a**) and at ~517 nm after the addition of 2 equiv of Cr^{3+} (**b**) to the solution containing **1** (10 μM) and different metal ions (20 μM).

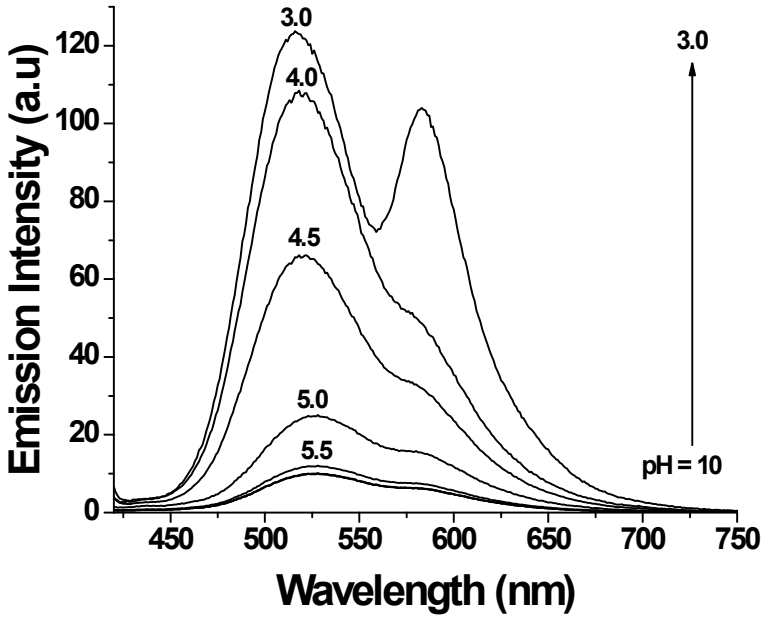

Fig. S10. pH dependant variations in fluorescence spectrum of **1** (10 μM)

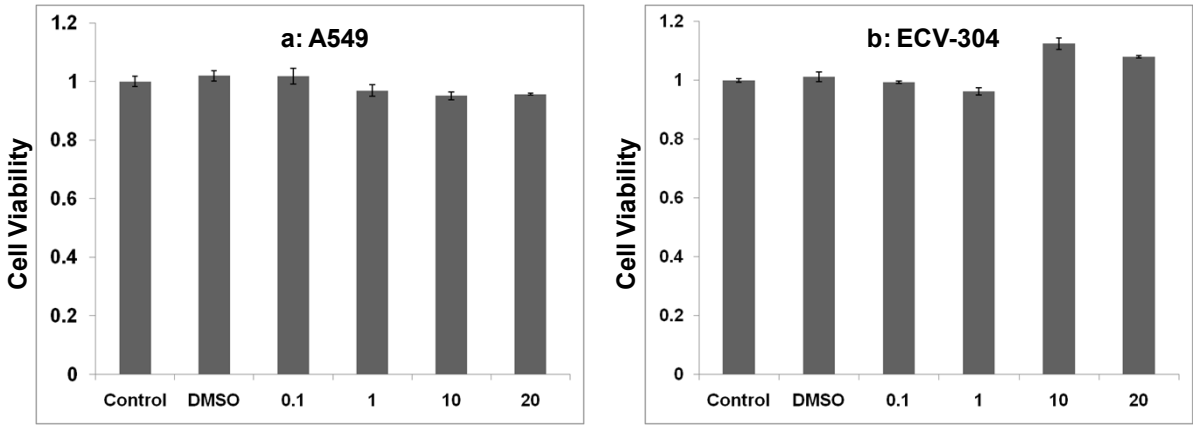

Fig. S11. Cell viability assay in (**a**) A549 and (**b**) ECV-304 cells using MTT reagent. Cells were incubated with probe **1** with a varied concentration (0.1 μM to 20 μM) for 48 h in A549 and ECV-304 cells. Results show that the probe **1** is biocompatible in A549 cells and ECV-304 up to 20 μM concentration.

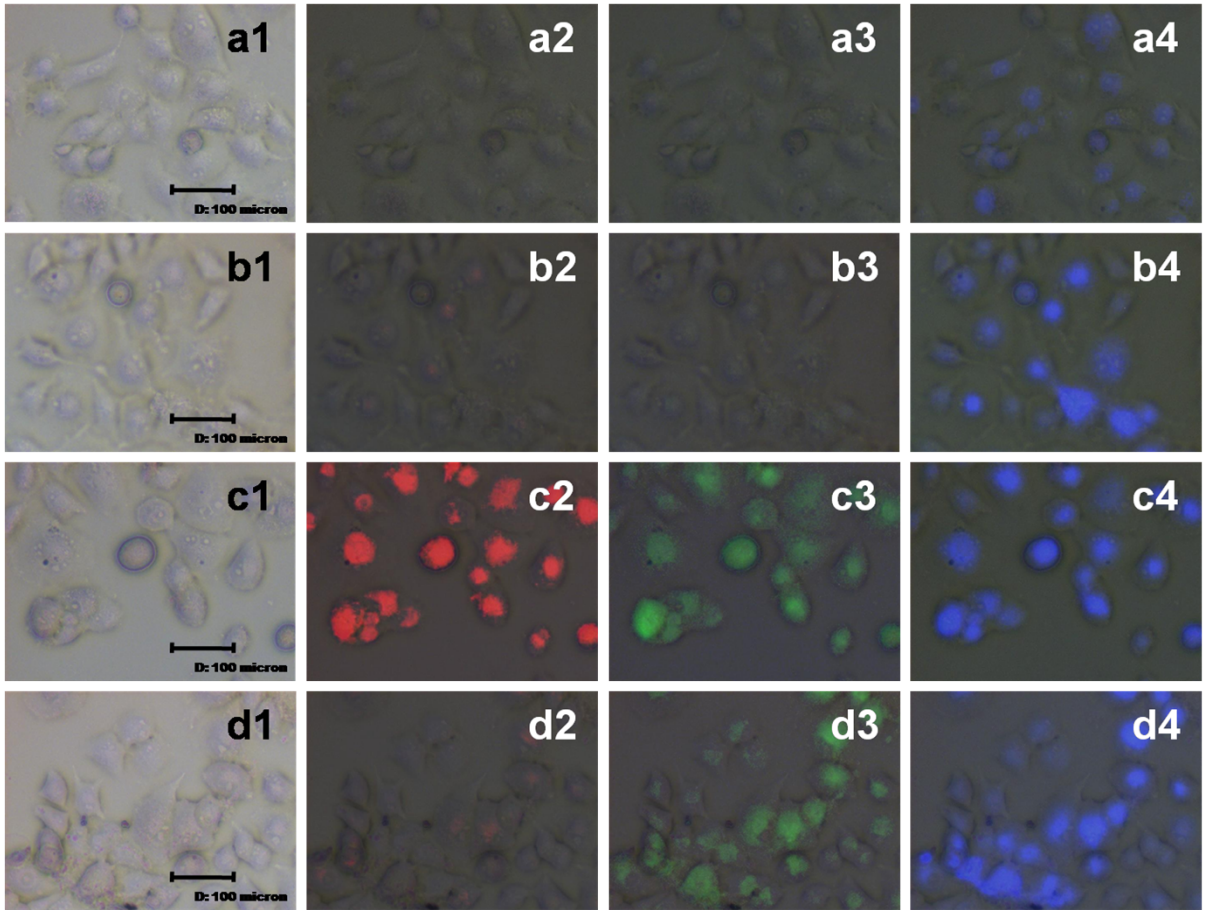

Fig. S12. Fluorescence microscopic images of A549 cells. Row 1 (**a1-a4**): untreated A549 cells, Row 2 (**b1-b4**): A549 cells treated with **2** (20 μM) alone; Row 3 (**c1-c4**): cells treated with **2** (20 μM) and Fe^{3+} (50 μM); Row 4 (**d1-d4**): cells treated with **2** (20 μM) and Cr^{3+} (50 μM). Column 1 (**a1–d1**): bright field images; Column 2 (**a2–d2**): merging of fluorescence red filter and bright field images; Column 3 (**a3-d3**): merging of fluorescence green filter and bright field images; and Column 4 (**a4–d4**): merging of bright field and blue Hoechst 33258 stained images of A549 cells.

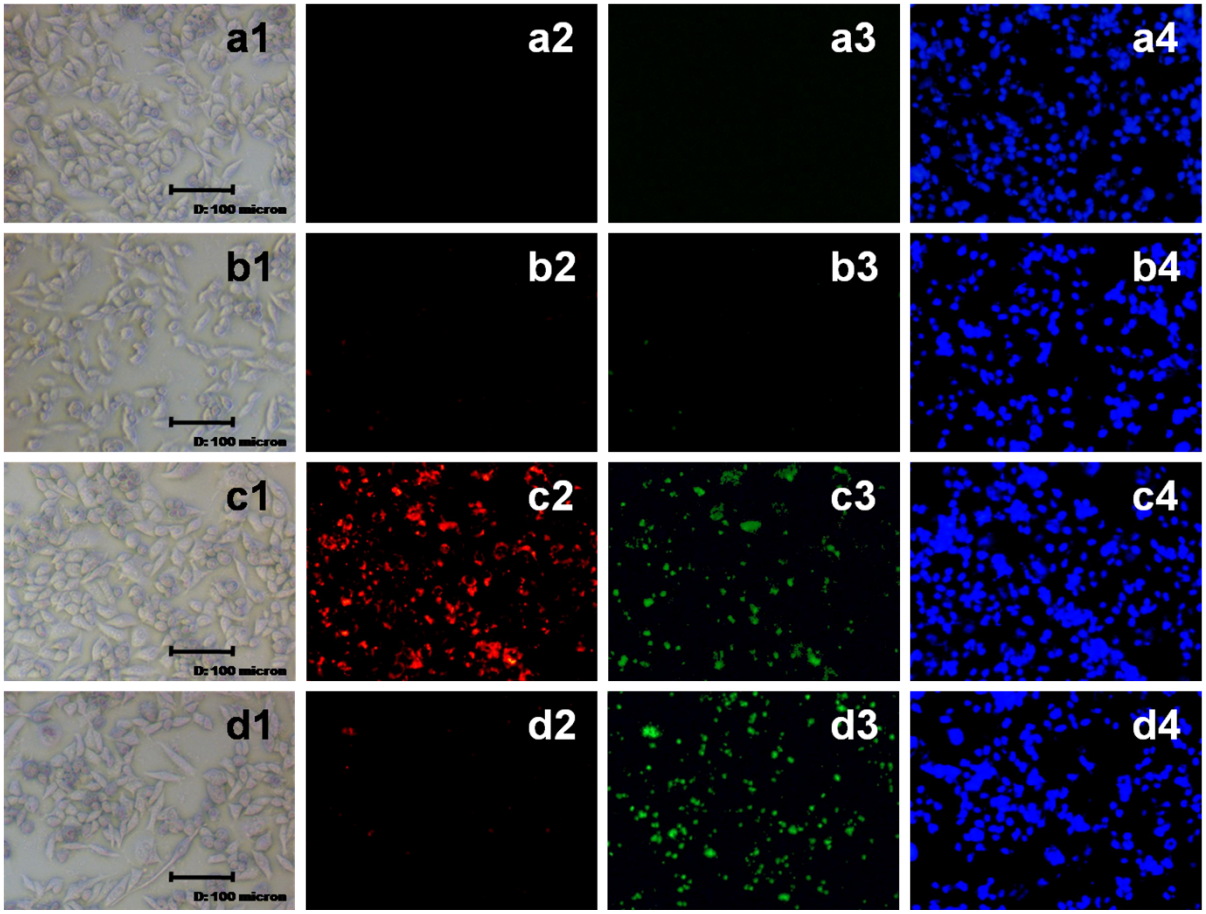

Fig. S13. Fluorescence microscopic images of CHO cells. Row 1 (**a1-a4**): untreated CHO cells, Row 2 (**b1-b4**): CHO cells treated with **1** (20 μM) alone; Row 3 (**c1-c4**): cells treated with **1** (20 μM) and Fe^{3+} (50 μM); Row 4 (d1-d4): cells treated with **1** (20 μM) and Cr^{3+} (50 μM). Column 1 (**a1–d1**): bright field images; Column 2 (**a2–d2**): fluorescence images with red filter; Column 3 (**a3-d3**): fluorescence images with green filter; and Column 4 (**a4–d4**): Hoechst 33258 stained images of CHO cells.

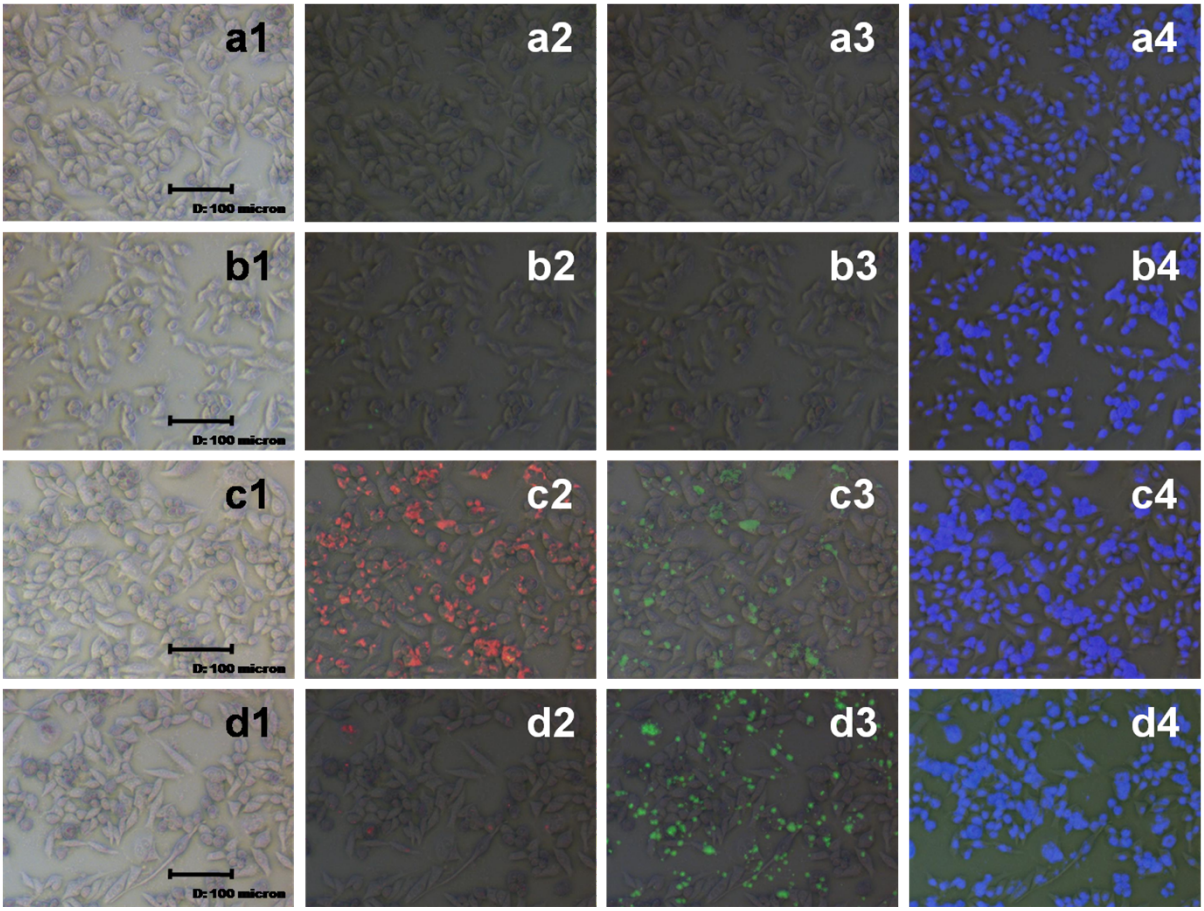

Fig. S14. Fluorescence microscopic images of CHO cells. Row 1 (**a1-a4**): untreated CHO cells, Row 2 (**b1-b4**): CHO cells treated with **2** (20 μM) alone; Row 3 (**c1-c4**): cells treated with **2** (20 μM) and Fe^{3+} (50 μM); Row 4 (**d1-d4**): cells treated with **2** (20 μM) and Cr^{3+} (50 μM). Column 1 (**a1–d1**): bright field images; Column 2 (**a2–d2**): merging of fluorescence red filter and bright field images; Column 3 (**a3-d3**): merging of fluorescence green filter and bright field images; and Column 4 (**a4–d4**): merging of bright field and blue Hoechst 33258 stained images of CHO cells.

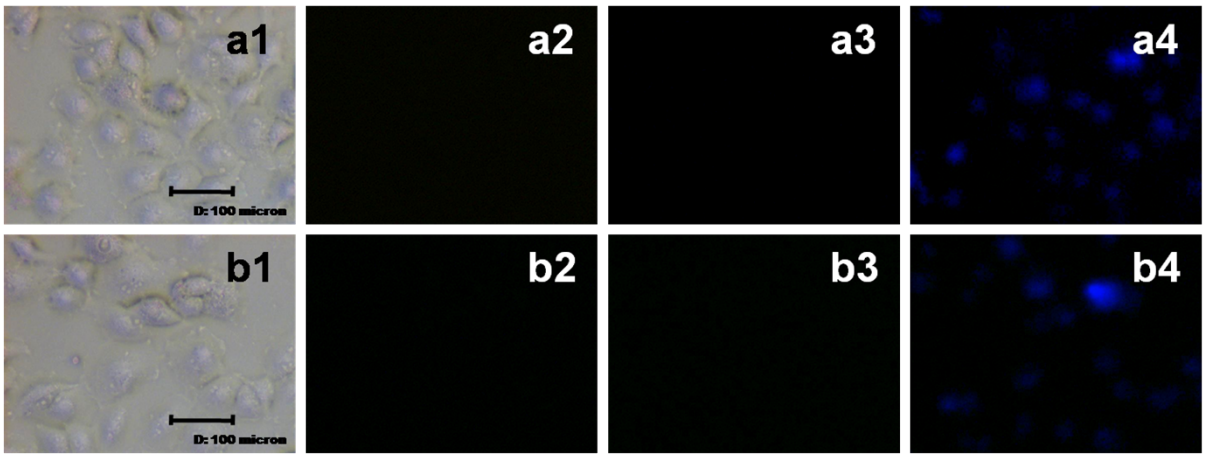

Fig. S15. Fluorescence microscopic images of A549 cells. Row 1: Cells treated with 50 µM Fe^{3+} (**a1-a4**). Row 2: Cells treated with 50 µM Cr^{3+} (**b1-b4**). Column 1: bright field images (**a1–b1**), Column 2: fluorescence images (**a2–b2**) with red filter, Column 3: fluorescence images (**a3-b3**) with green filter and Column 4: Hoechst 33258 stained images (**a4–b4**) of A549 cells.

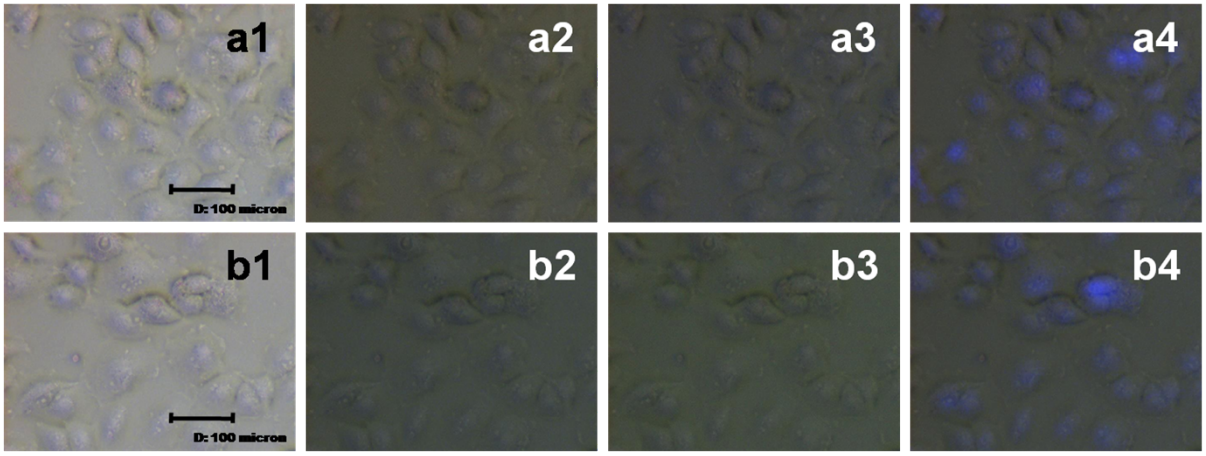

Fig. S16. Fluorescence microscopic images of A549 cells. Row 1 (**a1-a4**): cells treated with 50 µM Fe^{3+}. Row 2 (**b1-b4**): cells treated with 50 µM Cr^{3+}. Column 1(**a1–b1**): bright field images, Column 2 (**a2–b2**): merging of fluorescence red filter and bright field images, Column 3 (**a3-b3**): merging of fluorescence green filter and bright field images and Column 4 (**a4–b4**): merging of bright field and blue Hoechst 33258 stained images of A549 cells.

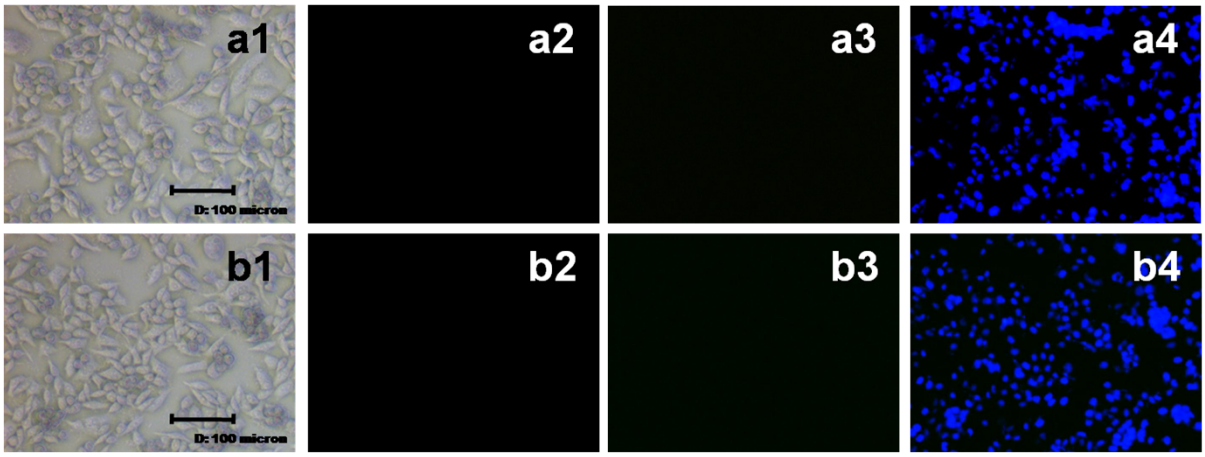

Fig. S17: Fluorescence microscopic images of CHO cells. Row 1: Cells treated with 50 µM Fe^{3+} (**a1-a4**). Row 2: Cells treated with 50 µM Cr^{3+} (**b1-b4**). Column 1: bright field images (**a1–b1**), Column 2: fluorescence images (**a2–b2**) with red filter, Column 3: fluorescence images (**a3-b3**) with green filter and Column 4: Hoechst 33258 stained images (**a4–b4**) of CHO cells.

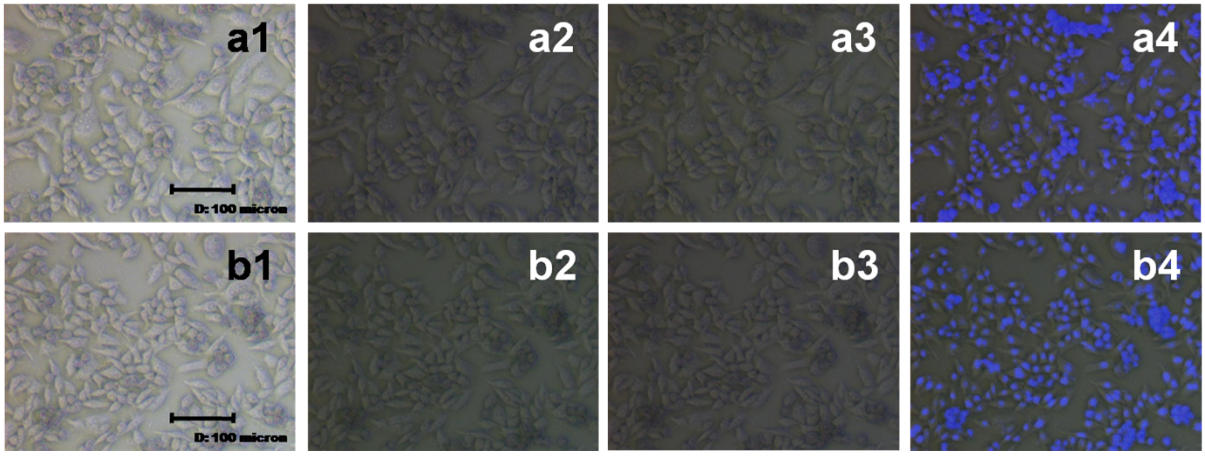

Fig. S18. Fluorescence microscopic images of CHO cells. Row 1 (**a1-a4**): cells treated with 50 µM Fe^{3+}. Row 2 (**b1-b4**): cells treated with 50 µM Cr^{3+}. Column 1(**a1–b1**): bright field images, Column 2 (**a2–b2**): merging of fluorescence red filter and bright field images, Column 3 (**a3-b3**): merging of fluorescence green filter and bright field images and Column 4 (**a4–b4**): merging of bright field and blue Hoechst 33258 stained images of CHO cells.

Reference

1. Y. Xiang and A. Tong, *Org. Lett*., 2006, **8**, 1549.

2. B. Wang, J. Hai, Z. Liu, Q. Wang, Z. Yang and S. Sun, *Angew. Chem. Int. Ed*., 2010, **49**, 4576.

3.A. J. Weerasinghe, C. Schmiesing, S. Varaganti, G. Ramakrishna and E. Sinn, *J. Phys. Chem. B,* 2010, **114**, 9413.

4. J. Mao, Q. He and W. Liu, *Talanta*, 2010, **80**, 2093.

5. A. Sikdar, S. S. Panja, P. Biswas and S. Roy, *J. Fluoresc*., 2012, **22**, 443.

6. M. Kaur, P. Kaur, V. Dhuna, S. Singh and K. Singh, *Dalton Trans*., DOI: 10.1039/c3dt53536c.

7. Z. Chen, L. Wang, G. Zou, M. Teng and J. Yu, *Chin. J. Chem*., 2012, **30**, 2844.

8. J. Li, C. Han, W. Wu, S. Zhang, J. Guo and H. Zhou, *New J. Chem*., 2014, **38**, 717

9. S. Goswami, A. K. Das, A. K. Maity, A. Manna, K. Aich, S. Maity, P. Saha and T. K. Mandal, *Dalton Trans*., 2014, **43**, 231.

10. A. Barba-Bon, A. M. Costero, S. Gil, M. Parra, J. Soto, R. Martınez-Manez and F. Sancenon, *Chem. Commun*., 2012, **48**, 3000.

11. I. Grabchev and D. Staneva, *Z. Naturforsch*., 2003, **58a**, 558.

12. N. R. Chereddy and S. Thennarasu, *Dyes Pigm*. 2011, **91**, 378.

13. L. Wang, J. S. Lau, C. R. Patra, Y. Cao, S. Bhattacharya, S. Dutta, D. Nandy, E. Wang, C. N. Rupasinghe, P. Vohra, M. R. Speller and D. Mukhopadhyay, *Molecular Cancer Research*, 2010, **8**, 1591; (b) T. J. Mosmann, *Immunol. Methods*, 1983, **65**, 55.

14. N. T. Patil, P. G. V. V. Lakshmi, B. Sridhar, S. Patra, M. Pal Bhadra, C. R. Patra, *Eur. J. Org. Chem.,* 2012, **9**, 1790.

15. A. Modak, A. K. Barui,C. R. Patra, A. Bhaumik, *Chem. Comm.* 2013, **49**, 7644.